Metastasis of clear cell renal cell carcinoma to hyalinizing trabecular tumor of the thyroid: A case report

CHUNJIAO LIU, HAIFEN MA, WEIHUA XIAO, JUNQIANG LI, MAOFEN JIANG and JINGDAN SHENG

Department of Pathology, Beilun District People's Hospital of Ningbo City, Ningbo, Zhejiang 315000, P.R. China

Received April 26, 2024; Accepted November 19, 2024

DOI: 10.3892/ol.2024.14851

Abstract. Renal cell carcinoma (RCC) is the most common malignancy that metastasizes to the thyroid; however, metastasis of RCC to a primary tumor of the thyroid is rare. The present study reports the case of RCC that had metastasized to the primary thyroid tumor; namely, a hyalinizing trabecular tumor (HTT). Notably, the RCC was resected 2 years prior. A 60-year-old female patient was referred to Ningbo Beilun District People's Hospital with radiographic findings indicating thyroid nodules. The patient's previous me`dical history included a left nephrectomy for the treatment of clear cell (cc)RCC in February 2021. No other distant metastases were identified as of the latest follow-up in April 2023. No abnormalities were observed during thyroid function tests prior to thyroid surgery. The surgical specimen appeared as a multinodular goiter with a solid nodule measuring 55x41x33 mm on the left lobe of the thyroid. Microscopic examination revealed a gray-yellow area inside the capsule of the largest nodule of the left lobe, which was composed of clear cells arranged in a solid pattern. Notably, tumor cells in other areas exhibited trabecular, nested and island patterns. Results of an immunohistochemical examination revealed that the clear cell lesion was negative for thyroid transcription factor-1 and calcitonin, and strongly positive for carbonic anhydrase IX, common acute lymphoblastic leukemia antigen and vimentin. To the best of our knowledge, the present study is the first to report a case of ccRCC that had metastasized to a HTT. A preliminary analysis of the potential mechanisms underlying ccRCC metastasis was performed. Following total thyroidectomy, the patient was treated with levothyroxine, underwent anti-programmed death-1 monoclonal antibody immunotherapy and small molecule tyrosine kinase inhibitor targeted therapy. An enhanced computed tomography scan revealed no evidence of metastatic disease to other organs. As of the latest follow-up, the patient was in a good condition with no sign of metastasis or recurrence.

Correspondence to: Ms. Chunjiao Liu, Department of Pathology, Beilun District People's Hospital of Ningbo City, 1288 Lushan East Road, Beilun, Ningbo, Zhejiang 315000, P.R. China
E-mail: liuchunjiao2022@163.com

Key words: clear cell renal cell carcinoma, hyalinizing trabecular tumor, immunohistochemistry

Introduction

Renal cell carcinoma (RCC) is a common malignant tumor of the urinary system, accounting for >85% of renal malignant tumors (1). The most common pathological type of RCC is clear cell (cc)RCC, which is a malignant tumor that arises from the renal parenchymal urinary tubular epithelial system. The clinical symptoms of early ccRCC are minimal and the minority of symptomatic patients exhibit different manifestations, such as abdominal pain, hematuria, weight loss or abdominal mass. In total, ~30% of patients present with metastases of varying severity and 25% of patients develop metastases following radical nephrectomy (2).

The prognosis of patients with early ccRCC is positive; however, in the advanced disease stage, ccRCC often invades surrounding nearby organs and metastasizes to the bloodstream. ccRCC commonly metastasizes to organs such as the lungs, bones, liver and brain (3-5). The prognosis of patients with metastatic ccRCC is poor, and the 5-year survival rate is ~9% (6,7). Metastasis of ccRCC to the thyroid gland, specifically within a primary thyroid tumor (PTT), is rare.

The results of a previous study have indicated that the average duration from radical nephrectomy to the diagnosis of ccRCC metastasis to the thyroid is 8.7 years (8). To the best of our knowledge, only 11 cases of ccRCC metastasizing to a PTT have been reported (5,9-17). These reports demonstrate that the immunohistochemical results of cells from metastatic ccRCC to PTT are typically negative for thyroglobulin, calcitonin and thyroid transcription factor 1 (TTF-1), and positive for common acute lymphoblastic leukemia antigen (CD10) and vimentin. Thyroid metastasis may be facilitated by hematogenous dissemination through the paravertebral venous network. However, the etiology underlying the phenomenon of metastasis from one tumor to another remains elusive (18).

Thyroid tumors are classified into primary and metastatic tumors. Metastatic tumors are less common compared with primary tumors. Primary tumors include thyroid papillary carcinoma, follicular carcinoma, medullary carcinoma and hyalinizing trabecular tumor (HTT). Notably, HTT of the thyroid gland is a rare primary tumor with a female predominance (19), which accounts for ~0.2% of PTTs (19). HTT was initially reported by Carney *et al* in 1987 (20), and

this tumor originates from the thyroid follicular epithelium. It is named for its stromal hyalinization and the trabecular and cord-like arrangement of the tumor. HTT often presents as a single, solid, well-defined nodule with a gray-yellow cut surface, medium texture and a fibrous capsule of varying thickness. HTT also exhibits unique histological features and protein expression level; for examples, the tumor cells of HTT are arranged in a trabecular pattern, with hyaline material visible between the trabecular cell nests, and the tumor cells are positive for TTF-1 and CD56 (21). As the observed nuclear characteristics and hyalinization are comparable with papillary thyroid carcinoma, HTT is often misdiagnosed via cytological examination using fine needle aspiration biopsy, leading to poor patient outcomes and further complications in tumor classification (22). In the early stages of the disease, no specific indicators are observed during clinical examination, only presentation with a thyroid nodule.

The present study presents a case of ccRCC metastasizing to a HTT of the thyroid.

Case report

In April 2023, a 60-year-old female was referred to Ningbo Beilun District People's Hospital (Ningbo, China) with radiographic findings indicating thyroid nodules. The previous medical history of the patient included a left radical nephrectomy in February 2021, performed for the treatment of ccRCC. Histological examination revealed grade 1 ccRCC (23), and no other distant metastases were observed during follow-up. As shown in Fig. 1A, preoperative thyroid ultrasound examination results indicated a hypoechoic nodule in the left lobe of the thyroid [Thyroid Imaging Reporting and Data System (TI-RADS) 4a] and a nodule in the right lobe of the thyroid (TI-RADS 3). TI-RADS is a classification level for thyroid nodules, where TI-RADS 4a indicates the presence of one of the following ultrasonographic malignant features: Extremely hypoechoic, microcalcifications or irregular microlobulated margins; the probability of malignancy in this category ranges from 5 to 10% (24). The results of computed tomography revealed enlargement of the left lobe of the thyroid with a mass-like low-density shadow inside, measuring ~40x32 mm (Fig. 1B). In addition, the left lobe exhibited poorly defined borders and an uneven density with visible calcifications inside the mass (Fig. 1B). Multiple small nodules were observed in the right lobe of the thyroid, with no abnormal density shadows observed in the isthmus of the thyroid. Notably, the patient did not present with enlarged lymph nodes on either side of the neck. The results of urine and blood tests were normal, and normal functioning of the thyroid and parathyroid was observed. Given the large size of the mass, there was a risk of tracheal deviation and compression. The patient's history of ccRCC and the potential for malignancy in the thyroid nodules was considered, and after the patient was informed, they refused fine needle aspiration cytology and opted for total thyroidectomy.

Specimens were surgically obtained via total thyroidectomy. Intraoperatively, diffuse enlargement of the left lobe of the thyroid was observed, along with multiple nodules with solid, clear borders. Notably, the largest nodule measured ~55x41x33 mm. Multiple nodules were also observed in the right lobe of the thyroid, with solid, clear borders, measuring ~24x14x11 mm. No nodules were observed in the isthmus.

Thyroidectomy specimens were fixed in 10% formalin for 48 h at 37˚C, routinely dehydrated, embedded in paraffin and cut into 4-μm sections. Subsequently, H&E staining was performed for 40 min at 37˚C, then the sections were examined under a light microscope (DM2000; Leica Microsystems, Inc.).

Immunohistochemical analyses were performed automatically using the Bench Mark ULTRA immunohistochemistry system (Ventana Medical Systems, Inc.), for which the paraffin-embedded tissues were sectioned (4 μm) using a paraffin slicing machine, mounted onto poly-L-lysine-coated glass slides and allowed to dry at 65˚C for 60 min. The sections were subsequently put into the immunohistochemistry instrument for automated antigen retrieval (pH 9.0 EDTA, 100˚C, 36 min) and blocking (3% hydrogen peroxide, 37˚C, 4 min), followed by incubation with primary antibodies and the secondary antibody, and chromogenic development. The sections were incubated with the following primary antibodies: Neural cell adhesion molecule (CD56; mouse; cat. no. MAB-0743), TTF-1 (mouse; cat. no. MAB-0599), cytokeratin 19 (CK19; mouse; cat. no. MAB-0829), chromogranin-A (CgA; rabbit; cat. no. RMA-0548), paired box 8 (PAX-8; mouse; cat. no. MAB-0837), carbonic anhydrase IX (CAIX; rabbit; cat. no. RAB-0615), CD10 (mouse; cat. no. MAB-0668), mucin-1 (MUC-1; mouse; cat. no. Kit-0011), cytokeratin 7 (CK7; mouse; cat. no. MAB-0828), Ki-67 (mouse; cat. no. MAB-0672) (all from Fuzhou Maixin Biotechnology Development Co., Ltd.) and BRAF-VE600E (mouse; cat. no. 790-5095; Roche Diagnostics) for 1 h at 37˚C. The bound primary antibody was detected using a ready-to-use secondary antibody (UltraView Universal DAB detection kit; cat. no. 760-500; Roche Diagnostics) for 36 min at 37˚C, and DAB (from the UltraView Universal DAB detection kit) was utilized as a chromogen for 8 min at 37˚C. After removing the sections from the instrument, they were immersed in distilled water containing detergent for washing and then rinsed with distilled water. Subsequently, the sections were dehydrated through a series of ethanol solutions and cleared with xylene before mounting the sections in an automated slide stainer. The sections were then ready to be observed under a microscope (Leica Microsystems, Inc. DM2000). A tumor measuring 55x41x33 mm was observed in the left thyroid tissue section. In addition, the tumor appeared gray-yellow in color, with areas of hemorrhage and a fibrous capsule on the periphery. A small area of ~8x5 mm was visible near the periphery of the tumor, with a multicolored appearance (Fig. 2A).

At a low magnification, the tumor boundary was clearly visible with a fibrous capsule (Fig. 2B). Tumor cells were composed of two histologically distinct cell types. In addition, the tumors exhibited solid growth with small beam- and nest-like structures, with transparent degeneration between the beams. Tumor cells were polygonal, fusiform, oval or elliptical in shape, with nuclear grooves, intranuclear pseudo-inclusions and small nucleoli. Rare nuclear division figures were observed (Fig. 3A). Microscopic examination also revealed that a number of tumor cells were located within the inner side of the capsule and arranged in a nest-like or glandular pattern. Regular reticular patterns were observed in the tumor and

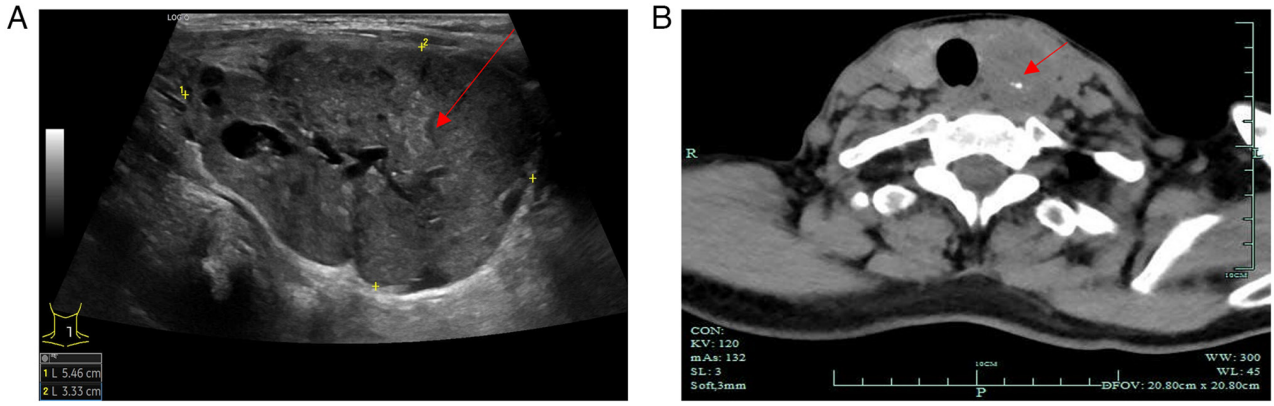

Figure 1. Ultrasound and computed tomography imaging of the thyroid. (A) Ultrasonography revealed a well-defined, hypoechoic mass (red arrow) with microcalcification, measuring 55x41x33 mm in the left lobe of the thyroid gland. (B) Computed tomography demonstrated that the left lobe of the thyroid gland was enlarged, with a mass-like area of low density (red arrow), measuring ~40x32 mm. Tumor density was heterogeneous with visible calcifications.

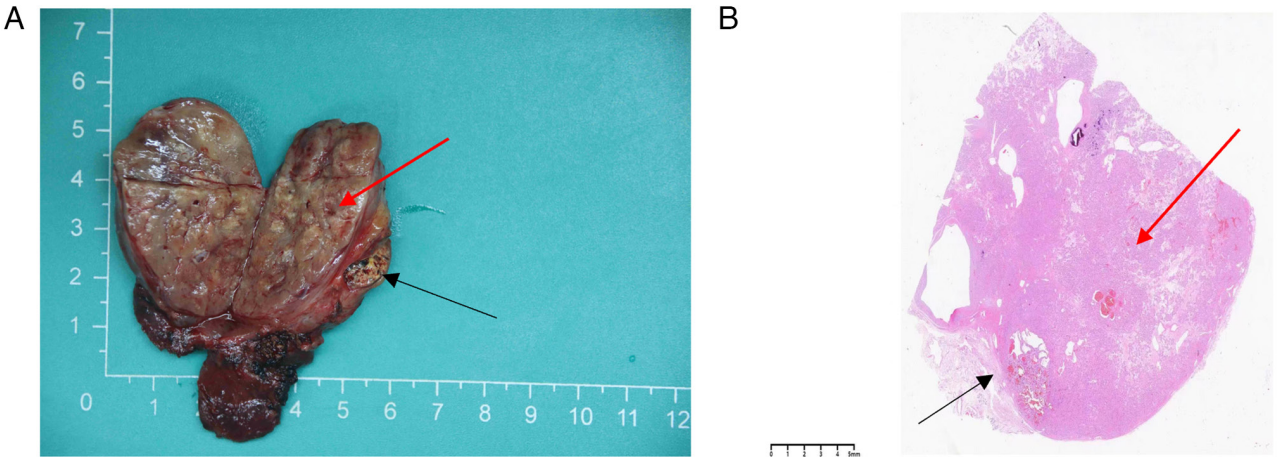

Figure 2. Gross appearance and morphology of tumor tissue. (A) Thyroid tissue sections exhibited a well-demarcated nodule with a pale brown appearance (red arrow) and a small golden-yellow nodule beneath the capsule of the nodule (black arrow). (B) H&E staining revealed two distinct histological patterns located within the capsule (black and red arrows; magnification, x4).

these were composed of small thin-walled blood vessels. The tumor cell cytoplasm was transparent, with clear capsules and circular nuclei, and the size was relatively uniform throughout. Results of the microscopic examination revealed nucleoli of several sizes, and acidophilic nucleoli (black arrow) were observed at x400 magnification (Fig. 3B).

Immunohistochemical analysis revealed that clear trabecular areas of the thyroid exhibited positive TTF-1 (Fig. 4A) and CD56 staining (Fig. 4B), whilst calcitonin (Fig. 4C), mesothelin (Fig. 4D), CK19 (Fig. 4E), BRAF-V600E (Fig. 4F) and CgA (Fig. 4G) expression was negative. Positivity for Ki-67 was <5% of tumor cells (Fig. 4H). By contrast, the clear cell areas exhibited positive PAX-8 (Fig. 5A), CAIX (Fig. 5B), CD10 (Fig. 5C), vimentin (Fig. 5D) and MUC-1 (Fig. 5E) expression, while CK7 (Fig. 5F) expression was negative. The observed histological features and immune profile were consistent with metastatic ccRCC to the thyroid, with clear cell changes in the lamellar tumor.

In the present case, the patient was diagnosed with metastatic ccRCC to a HTT of the thyroid. Following surgery, the patient received levothyroxine therapy, with a regimen of 75 μg levothyroxine sodium tablets taken orally once daily, 1 h before breakfast. Thyroid function was followed up every 3 months to serve as the basis for dosage adjustment. she also underwent an enhanced computed tomography scan, which indicated that no metastasis to other organs had occurred (Fig. 6). The lungs and mediastinum (Fig. 6A), liver, gallbladder and stomach (Fig. 6B), intestinal tract and right kidney (Fig. 6C), as well as the uterus, bilateral adnexa and bladder (Fig. 6D), all showed no evidence of tumorous lesions. From May 18, 2023 to the present date, the patient has undergone programmed death-1 monoclonal antibody immunotherapy and small molecule tyrosine kinase inhibitor targeted therapy. As of the latest visit (October 2024), the patient was in a good condition with no sign of metastasis or recurrence, and regular follow-ups every 3 months have been arranged.

Discussion

Most patients with metastatic ccRCC to the thyroid present with painless masses, which are often misdiagnosed as a nodular goiter. Clinical symptoms associated with nodular goiters include dysphagia, respiratory distress, hoarseness, neck pain and a cough (25). In the present case, the patient

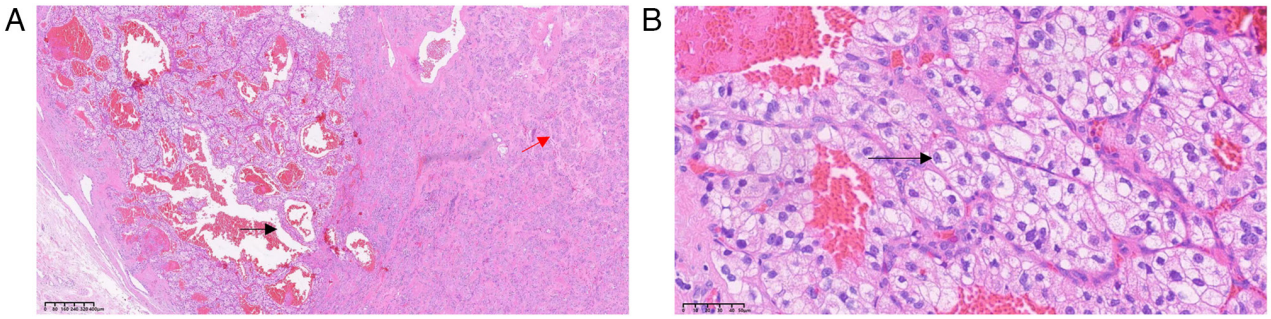

Figure 3. Histological features of tumor tissue at high magnification (magnification, x400). (A) The tumor exhibited two distinct histological patterns. On the right side, the tumor cells were arranged in a trabecular pattern, with eosinophilic and hyaline material (red arrow) visible between the trabeculae and the tumor cells. On the left side, the tumor was arranged in a nested pattern, composed of clear cells (black arrow). (B) The cytoplasm of the clear tumor cells was transparent with well-defined capsules. Cell nuclei were relatively uniform in size, with nucleoli that varied in size. In addition, a rich vascular background was observed in the stroma. Results were obtained using H&E staining.

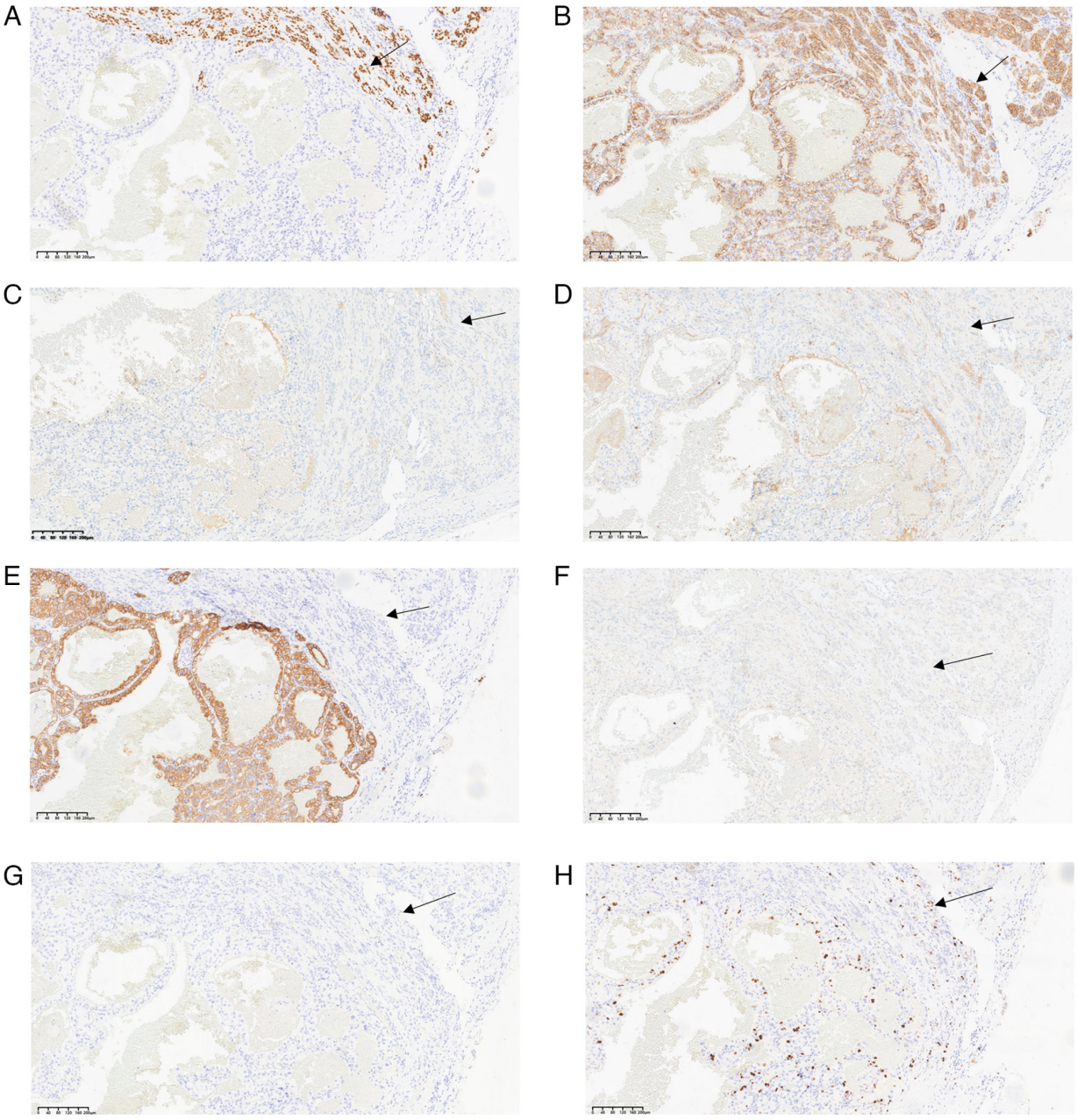

Figure 4. Immunohistochemical results of the clear trabecular area (magnification, x100). There was positive expression of (A) thyroid transcription factor-1 and (B) neural cell adhesion molecules, and negative expression of (C) calcitonin, (D) mesothelin, (E) cytokeratin 19, (F) BRAF-V600E and (G) chromogranin-A. (H) Ki-67 staining revealed a proliferative index of <5% (black arrows).

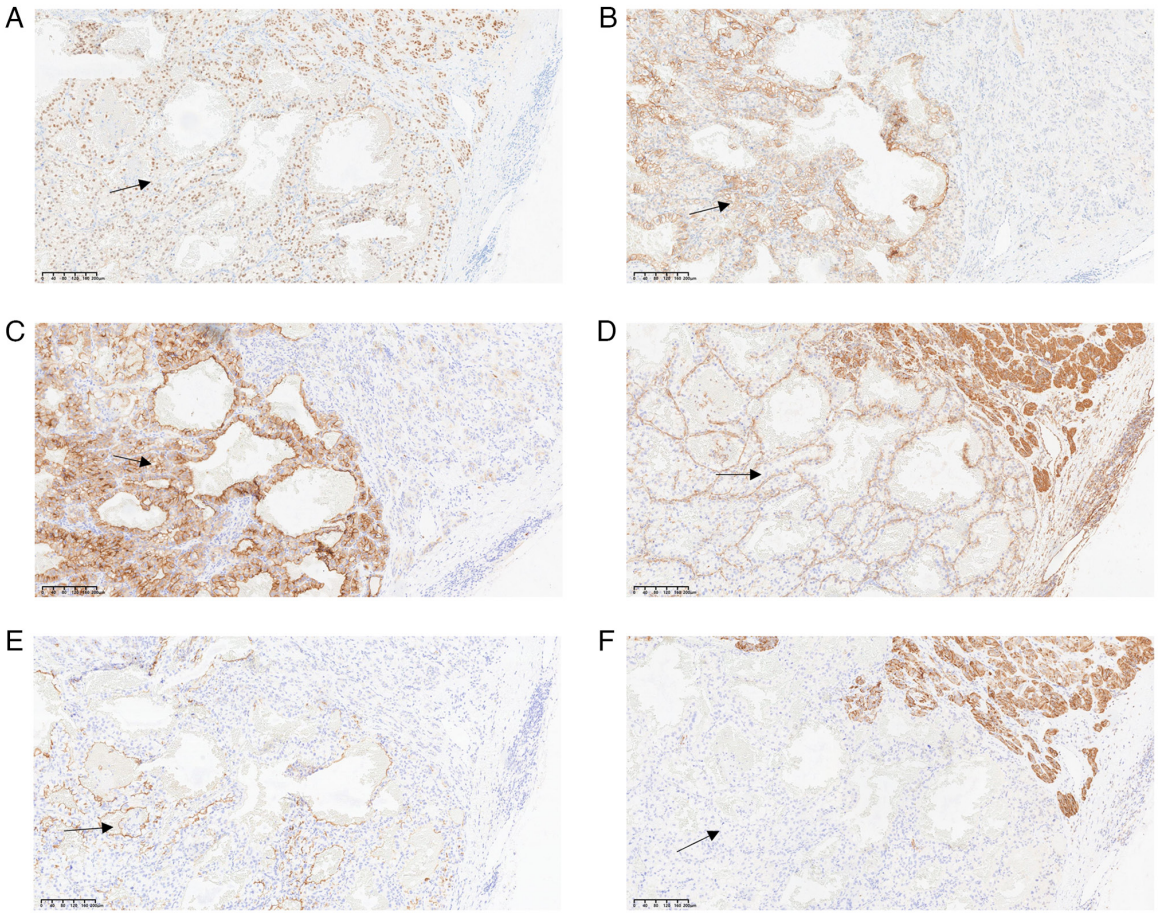

Figure 5. Immunohistochemical results of the clear cell area (magnification, x100).There was positive expression of (A) paired box 8, (B) positive carbonic anhydrase IX, (C) common acute lymphoblastic leukemia antigen, (D) vimentin and (E) mucin1. (F) There was negative expression of cytokeratin 7 (black arrows).

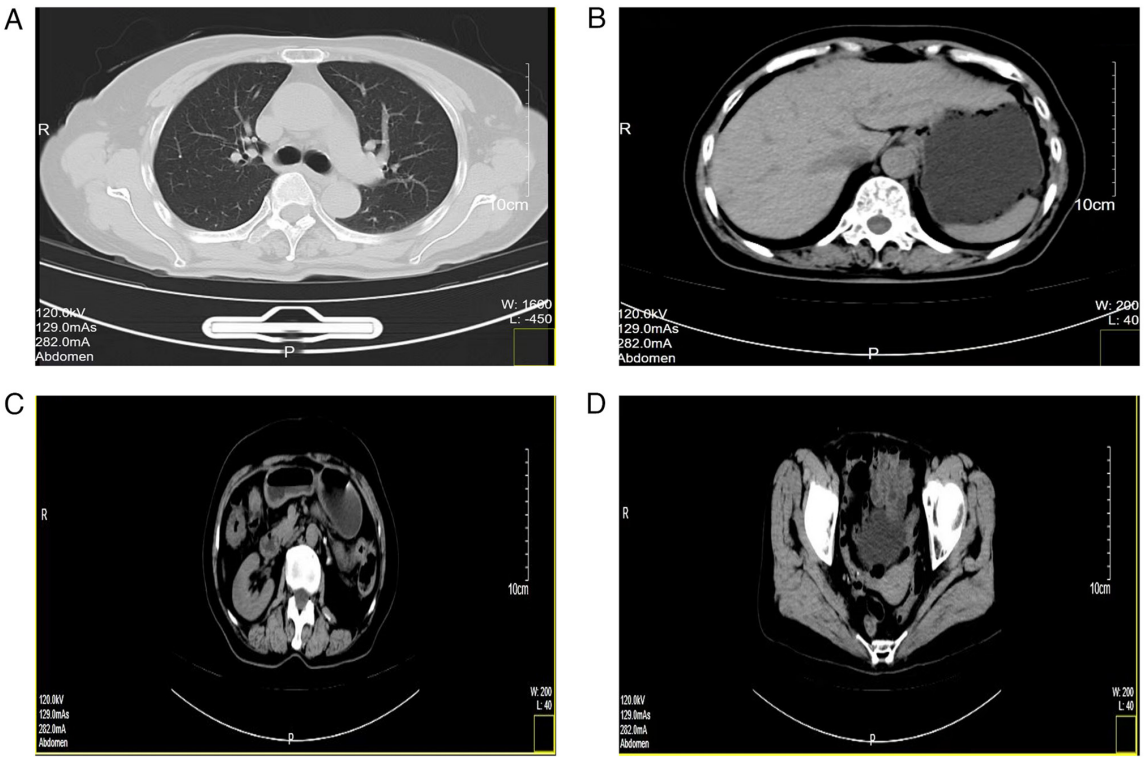

Figure 6. Enhanced computed tomography of the chest, abdomen and pelvic regions 15 months post-surgery indicated no mass lesions. Representative images of the (A) lungs and mediastinum, (B) liver, gallbladder and stomach, (C) intestinal tract and right kidney and (D) uterus, bilateral adnexa and bladder.

presented with a painless cervical mass and no additional clinical symptoms. Notably, diagnosis of metastatic ccRCC to the thyroid remains challenging, due to the reliance on H&E staining. Using imaging, metastatic ccRCC to the thyroid typically appears as a single nodule, which may be misdiagnosed as a primary tumor. During diagnosis of PTTs, HTTs of the thyroid may be misdiagnosed as medullary thyroid carcinoma, follicular adenoma or paraganglioma. Notably, immunohistochemistry and molecular testing are commonly used to distinguish between them (26). Specific tumor markers aid in determining the primary site of the metastatic tumor, for example, calcitonin is a specific marker for medullary thyroid carcinoma (27) and CAIX is a specific marker for ccRCC (28). Immunohistochemical analysis of the tumor revealed positive TTF-1 expression, which verified the presence of a PTT. Moreover, negative CK19, CgA and BRAF-V600E expression and positive CD56 expression, in combination with positive periodic acid-Schiff staining in the stroma, was indicative of a HTT of the thyroid gland. Subsequently, the primary objective was to determine the specific type of clear cell area within the tumor. The following markers were utilized: PAX-8, CAIX, CD10, CK7, MUC-1 and vimentin. Notably, CK7 exhibited negative expression, whilst CAIX, CD10, PAX-8, MUC-1 and vimentin all demonstrated positive expression. These findings had led to the diagnosis of the clear cell area as ccRCC.

In the diagnosis of RCC, to differentiate and distinguish between types, transcription factor 3 (TFE3) is commonly used for diagnosing TFE3 rearranged RCC (29,30); fumarate hydratase (FH) is used for diagnosing FH-deficient RCC (29,30); and cytokeratin (CK) is used as an auxiliary diagnostic tool for ccRCC (29). When CAIX, CD10, PAX-8 and vimentin all exhibit positive expression, the CK marker can be omitted. Consequently, it seemed that it was unnecessary to employ additional markers such as CK, TFE3 and FH for further characterization in the present study.

Collectively, immunohistochemical expression levels, the patient's medical history and H&E staining were used to verify ccRCC metastasis to a HTT of the thyroid. In clinical pathology, when tumor tissues outside the kidney exhibit morphological features similar to those of ccRCC, the aforementioned immunohistochemical markers can be used to assist in diagnosis.

In the 11 previously reported cases of ccRCC metastases to PTTs, there were four instances of the follicular variant of papillary thyroid carcinoma (9-12), four cases of follicular adenoma (5,13-15), one case of papillary thyroid carcinoma (16), one case of Hurthle cell (oncocytic) carcinoma (15) and one case of Hurthle cell adenoma (17). Although all cases were metastatic to thyroid tumors following ccRCC-mediated radical nephrectomy, the histological features and biological behaviors of the tumor included in the present study differed from those previously reported. Among the 11 cases reported, there were 4 cases of follicular adenoma and 1 case of Hurthle cell adenoma, both of which were benign tumors. The morphology of their tumor tissues was characterized by complete encapsulation. However, they also exhibited certain distinct features. Specifically, Hurthle cell adenoma presented with abundant granules in the eosinophilic cytoplasm, whilst follicular adenoma displayed cells arranged in follicles of varying sizes. None of these five cases showed metastasis to other organs. The remaining six cases were malignant tumors. The follicular variant of papillary thyroid carcinoma displayed follicles of varying sizes and shared characteristics with papillary thyroid carcinoma cells. Both Hurthle cell (oncocytic) carcinoma and papillary thyroid carcinoma demonstrated invasive growth. Among these malignant cases, four cases exhibited metastasis to other organs, including the liver, pancreas, contralateral kidney, spine and subcutaneous tissue. In the present case, the tumor cell exhibited unique clear cell alterations with hyaline stroma, which was different from previously reported cases. The biological behavior of the tumor was intermediate between that of benign and malignant tumors, showing differences from both.

Few studies have focused on the mechanisms underlying metastatic ccRCC to the thyroid. The rarity of this tumor may be due to high levels of oxygen and iodine as a result of abundant blood flow in the thyroid (31). In diseases such as chronic thyroiditis or nodular goiter, the oxygen and iodine content in the thyroid decreases, leading to higher levels of metastasis to the thyroid (32-34). In a previous study, a metabolic hypothesis was proposed, also known as the 'seed and soil' hypothesis. This hypothesis emphasizes the interaction between tumor cells (seeds) and the microenvironment of the target organ for metastasis (soil). This theory denotes that the metastasis and growth of tumor cells are not only determined by the biological characteristics of the tumor cells themselves but are also influenced by the microenvironment of the target organ (5). In addition, a mechanical hypothesis was proposed, which suggested that tumor cells metastasize to other tumor tissues through the circulatory system, where they colonize and grow. During metastasis, tumor cells may easily invade the recipient tumor tissue due to an abundant vascular supply (35). The interstitium of a HTT contains an abundant microvascular network (36), and this rich vascular network not only provides nutrients and oxygen for metastatic tumor cells, but also alters the microenvironment of the recipient tumor cells (9). Moreover, the abundant vascular network may also alter the micromechanical environment of the recipient tumor cell matrix, and such changes may promote the metastasis of tumor cells (37). The mechanism underlying ccRCC metastasis to an HTT is complex, and both metabolic and mechanical hypotheses are valid. However, further investigations are required to determine the specific mechanisms involved.

Treatment of metastatic thyroid tumors may include surgery, radiotherapy or chemotherapy. Surgical intervention is the primary integrative therapeutic approach, involving total or partial thyroidectomy, along with cervical lymph node dissection. Following surgery, patients are treated with long-term oral thyroid hormone replacement therapy (38). Thyroidectomy is considered a more effective treatment option than radiotherapy and chemotherapy (39). However, there is ongoing debate regarding the surgical management of metastatic thyroid tumors. In cases involving unilateral nodules, unilateral thyroidectomy is favored to minimize damage to the recurrent laryngeal nerve and parathyroid glands (40). However, patients that undergo total thyroidectomy exhibit a lower rate of recurrence (41). For patients with multiple and small bilateral lesions, total thyroidectomy may be recommended to prevent relapse (42). Determining the appropriate

surgical approach for patients requires a comprehensive assessment by the clinician, for the development of an individualized treatment plan.

In conclusion, metastasis of ccRCC to a HTT is rare, with clinical manifestations that are not specific to the tumor type, leading to challenges in clinical diagnosis. Accurate pathological diagnosis combined with clinical information and immunohistochemical analysis are crucial for the development of an individualized treatment plan.

Acknowledgements

Not applicable.

Funding

No funding was received.

Availability of data and materials

The data generated in the present study may be requested from the corresponding author.

Authors' contributions

CL contributed to the study design, writing and revisions of the present study. MJ and JL were responsible for drafting the manuscript and analysing disease mechanisms. HM and WX were responsible for the case analysis and pathological diagnosis assistance. JS was responsible for the sampling of surgical specimens and immunohistochemical analysis, and made key revisions to the content of the manuscript and. CL and MJ confirm the authenticity of all the raw data. All authors have read and approved the final version of the manuscript.

Ethics approval and consent for participation

The present study was approved by the Beilun District People's Hospital Medical Ethics Committee (Ningbo, China; April 23, 2024; approval no. 2024LP023). Written informed consent was obtained from the patient, prior to investigations using tumor samples.

Patient consent for publication

Written informed consent for the publication of this article was obtained from the patient.

Competing interests

The authors declare that they have no competing interests.

References

1. Deng FM and Melamed J: Histologic variants of renal cell carcinoma: Does tumor type influence outcome? Urol Clin North Am 39: 119-132, 2012.
2. Leibovich BC, Blute ML, Cheville JC, Lohse CM, Frank I, Kwon ED, Weaver AL, Parker AS and Zincke H: Prediction of progression after radical nephrectomy for patients with clear cell renal cell carcinoma: A stratification tool for prospective clinical trials. Cancer 97: 1663-1671, 2003.
3. Bianchi M, Sun M, Jeldres C, Shariat SF, Trinh QD, Briganti A, Tian Z, Schmitges J, Graefen M, Perrotte P, *et al*: Distribution of metastatic sites in renal cell carcinoma: A population-based analysis. Ann Oncol 23: 973-980, 2012.
4. Xue J, Chen W, Xu W, Xu Z, Li X, Qi F and Wang Z: Patterns of distant metastases in patients with clear cell renal cell carcinoma-A population-based analysis. Cancer Med 10: 173-187, 2021.
5. Koo HL, Jang J, Hong SJ, Shong Y and Gong G: Renal cell carcinoma metastatic to follicular adenoma of the thyroid gland. A case report. Acta Cytol 48: 64-68, 2004.
6. Tsimafeyeu I, Zolotareva T, Varlamov S, Zukov R, Petkau V, Mazhbich M, Statsenko G, Safina S, Zaitsev I, Sakaeva D, *et al*: Five-year survival of patients with metastatic renal cell carcinoma in the Russian federation: Results from the RENSUR5 registry. Clin Genitourin Cancer 15: e1069-e1072, 2017.
7. Walton J, Ng ASN, Arevalo K, Apostoli A, Meens J, Karamboulas C, St-Germain J, Prinos P, Dmytryshyn J, Chen E, *et al*: PRMT1 inhibition perturbs RNA metabolism and induces DNA damage in clear cell renal cell carcinoma. Nat Commun 15: 8232, 2024.
8. Khaddour K, Marernych N, Ward WL, Liu J and Pappa T: Characteristics of clear cell renal cell carcinoma metastases to the thyroid gland: A systematic review. World J Clin Cases 7: 3474-3485, 2019.
9. Badawi F and Meliti A: Tumor-to-tumor metastasis of renal cell carcinoma to a follicular variant of papillary thyroid carcinoma: A case report and literature review. Cureus 14: e23742, 2022.
10. Baloch ZW and LiVolsi VA: Tumor-to-tumor metastasis to follicular variant of papillary carcinoma of thyroid. Arch Pathol Lab Med 123: 703-706, 1999.
11. Kefeli M and Mete O: An unusual solitary thyroid nodule with bloody follicles: Metastatic renal cell carcinoma within an infiltrative follicular variant papillary carcinoma. Endocr Pathol 27: 171-174, 2016.
12. Yu J, Nikiforova MN, Hodak SP, Yim JH, Cai G, Walls A, Nikiforov YE and Seethala RR: Tumor-to-tumor metastases to follicular variant of papillary thyroid carcinoma: histologic, immunohistochemical, and molecular studies of two unusual cases. Endocr Pathol 20: 235-242, 2009.
13. Wolf G, Aigner RM, Humer-Fuchs U, Schwarz T, Krippl P and Wehrschuetz M: Renal cell carcinoma metastasis in a microfollicular adenoma of the thyroid gland. Acta Med Austriaca 29: 141-142, 2002 (In German).
14. Medas F, Calò PG, Lai ML, Tuveri M, Pisano G and Nicolosi A: Renal cell carcinoma metastasis to thyroid tumor: A case report and review of the literature. J Med Case Rep 7: 265, 2013.
15. Ryska A and Cáp J: Tumor-to-tumor metastasis of renal cell carcinoma into oncocytic carcinoma of the thyroid. Report of a case and review of the literature. Pathol Res Pract 199: 101-106, 2003.
16. Bohn OL, De las Casas LE and Leon ME: Tumor-to-tumor metastasis: Renal cell carcinoma metastatic to papillary carcinoma of thyroid-report of a case and review of the literature. Head Neck Pathol 3: 327-330, 2009.
17. Qian L, Pucci R, Castro CY and Eltorky MA: Renal cell carcinoma metastatic to Hurthle cell adenoma of thyroid. Ann Diagn Pathol 8: 305-308, 2004.
18. Tjahjono R, Phung D, Gurney H, Gupta R, Riffat F and Palme CE: Thyroid gland metastasis from renal cell carcinoma: A case series and literature review. ANZ J Surg 91: 708-715, 2021.
19. Lee S, Han BK, Ko EY, Oh YL, Choe JH and Shin JH: The ultrasonography features of hyalinizing trabecular tumor of the thyroid are more consistent with its benign behavior than cytology or frozen section readings. Thyroid 21: 253-259, 2011.
20. Carney JA, Ryan J and Goellner JR: Hyalinizing trabecular adenoma of the thyroid gland. Am J Surg Pathol 11: 583-591, 1987.
21. Liu Y, Huang X, Hu Y, Wang F, Du T, He W, Chen L, Lang B, Pu Q and Chen H: Hyalinizing trabecular tumor of the thyroid: a clinicopathological analysis of four cases and review of the literature. Int J Clin Exp Pathol 10: 7616-7626, 2017.
22. Howard BE, Gnagi SH, Ocal IT and Hinni ML: Hyalinizing trabecular tumor masquerading as papillary thyroid carcinoma on fine-needle aspiration. ORL J Otorhinolaryngol Relat Spec 75: 309-313, 2013.
23. Warren AY and Harrison D: WHO/ISUP classification, grading and pathological staging of renal cell carcinoma: Standards and controversies. World J Urol 36: 1913-1926, 2018.

24. Malhi HS and Grant EG: Ultrasound of thyroid nodules and the thyroid imaging reporting and data system. Neuroimaging Clin N Am 31: 285-300, 2021.
25. Tang Q and Wang Z: Metastases to the thyroid gland: What can we do? Cancers (Basel) 14: 3017, 2022.
26. Chu S: Hyalinizing trabecular tumor of the thyroid: A case report. Asian J Surg 46: 5559-5560, 2023.
27. Feng J and Wang J: Expression and clinical significance of Ki67 and calcitonin in medullary thyroid carcinoma. Lin Chuang Er Bi Yan Hou Tou Jing Wai Ke Za Zhi 28: 1921-1924, 2014 (In Chinese).
28. Luong-Player A, Liu H, Wang HL and Lin F: Immunohistochemical reevaluation of carbonic anhydrase IX (CA IX) expression in tumors and normal tissues. Am J Clin Pathol 141: 219-225, 2014.
29. Mahmut A and Sean RW: Immunohistochemistry for the diagnosis of renal epithelial neoplasms. Semin Diagn Pathol 39: 1-16, 2022.
30. Kanakaraj J, Chang J, Hampton LJ and Smith SC: The New WHO category of 'molecularly defined renal carcinomas': clinical and diagnostic features and management implications. Urol Oncol 42: 211-219, 2024.
31. Cilengir AH, Kalayci TO, Duygulu G, Rezanko TA and İnci MF: Metastasis of renal clear cell carcinoma to thyroid gland mimicking adenomatous goiter. Pol J Radiol 81: 618-621, 2016.
32. Zivaljevic V, Jovanovic M, Perunicic V and Paunovic I: Surgical treatment of metastasis to the thyroid gland: A single center experience and literature review. Hippokratia 22: 137-140, 2018.
33. Mohammadi A, Toomatari SB and Ghasemi-Rad M: Metastasis from renal cell carcinoma to thyroid presenting as rapidly growing neck mass. Int J Surg Case Rep 5: 1110-1112, 2014.
34. Cordes M and Kuwert T: Metastases of non-thyroidal tumors to the thyroid gland: A regional survey in middle franconia. Exp Clin Endocrinol Diabetes 122: 273-276, 2014.
35. Fidler IJ: The pathogenesis of cancer metastasis: The 'seed and soil' hypothesis revisited. Nat Rev Cancer 3: 453-458, 2003.
36. Carney JA, Hirokawa M, Lloyd RV, Papotti M and Sebo TJ: Hyalinizing trabecular tumors of the thyroid gland are almost all benign. Am J Surg Pathol 32: 1877-1889, 2008.
37. Neophytou CM, Panagi M, Stylianopoulos T and Papageorgis P: The role of tumor microenvironment in cancer metastasis: Molecular mechanisms and therapeutic opportunities. Cancers (Basel) 13: 2053, 2021.
38. Cao J, Yu YE, Li NN, Wu YX, Shi JN and Fang MY: Thyroid metastasis from non-small cell lung cancer. Int J Clin Exp Pathol 12: 3013-3021, 2019.
39. Straccia P, Mosseri C, Brunelli C, Rossi ED, Lombardi CP, Pontecorvi A and Fadda G: Diagnosis and treatment of metastases to the thyroid gland: A meta-analysis. Endocr Pathol 28: 112-120, 2017.
40. Nixon IJ, Coca-Pelaz A, Kaleva AI, Triantafyllou A, Angelos P, Owen RP, Rinaldo A, Shaha AR, Silver CE and Ferlito A: Metastasis to the Thyroid Gland: A Critical Review. Ann Surg Oncol 24: 1533-1539, 2017.
41. Russell JO, Yan K, Burkey B and Scharpf J: Nonthyroid metastasis to the thyroid gland: Case series and review with observations by primary pathology. Otolaryngol Head Neck Surg 155: 961-968, 2016.
42. Iesalnieks I, Winter H, Bareck E, Sotiropoulos GC, Goretzki PE, Klinkhammer-Schalke M, Bröckner S, Trupka A, Anthuber M, Rupprecht H, *et al*: Thyroid metastases of renal cell carcinoma: Clinical course in 45 patients undergoing surgery. Assessment of factors affecting patients' survival. Thyroid 18: 615-624, 2008.